

Phloem loading in the sucrose-export-defective (*SXD-1*) mutant maize is limited by callose deposition at plasmodesmata in bundle sheath-vascular parenchyma interface

C. E. J. Botha, R. H. M. Cross, A. J. E. van Bel, and C. I. Peter

Summary. Using Lucifer Yellow we have demonstrated that the phloem-loading pathway from the mesophyll to the bundle sheath-vascular parenchyma interface in *Zea mays* source leaves follows a symplasmic route in small and intermediate vascular bundles in control as well as in the green sections of mutant sucrose-export-defective (*SXD-1*) plants. In the anthocyanin-rich mutant leaf sections, Lucifer Yellow transport was prohibited along the same path, at the bundle sheath-vascular parenchyma interface in particular. Plasmodesmata at the latter interface in *SXD-1* anthocyanin-rich leaf sections appear to be structurally altered through callose deposition at the plasmodesmal orifices. We suggest that a transport bottleneck at the bundle sheath-vascular parenchyma interface is thus orchestrated and regulated through callose formation, preventing symplasmic transport across this important loading interface.

Keywords: Callose; Lucifer yellow; Plasmodesma; Phloem loading; Sucrose-export-defective mutant; *Zea mays*.

Introduction

Debate continues on the mode of phloem loading in higher plants, but there is general agreement that the loading process is either symplasmic, apoplasmic, or mixed-mode symplasmic and apoplasmic (Gamalei 1989,1991; Turgeon and Beebe 1991; Russin et al. 1996; and references therein). It is clear that neither an entirely apoplasmic nor symplasmic route could, or should, be considered as universal (van Bel 1992, 1993).

It is now accepted that the assimilate transport pathway from the mesophyll to the interface of bundle sheath (BS) and vascular parenchyma (VP) cells in source leaves of grasses follows a symplasmic route (see Botha and Cross 1997 and references therein). It is usually at interfaces internal to this, for example, at the boundary between the VP and the companion cell-sieve tube complex that we find evidence for symplasmic discontinuity and hence a potential apoplasmic loading step in all grass species examined to date. Furthermore, the different bundle orders within the blades of both C³ and C⁴ grasses have largely different functions (Evert et al. 1996, and references in Botha and Cross 1997). For example, the small and intermediate bundles in barley have been implicated in assimilate loading, whilst the large bundles are associated with longitudinal transport (Evert et al. 1996).

Maize is an intensely studied plant, and there is a comprehensive knowledge base concerning its vasculature and ultrastructure (Evert et al. 1977, 1978; Russin et al. 1996; and references therein). Maize is a C⁴ NADP-Me species and has a high rate of photosynthesis (Kalt-Torres 1987), which requires that the incorporated carbon within the mesophyll be rapidly transported into the BS, where malate decarboxylation and the assimilation of the carbon into sucrose occur. Sucrose in turn must be rapidly transported via plasmodesmata down a symplasmic gradient, along the cell loading pathway from the Kranz mesophyll (KMS) to the VP which, by inference, should be able to support high rates of solute movement through presumed unoccluded plasmodesmata, terminating at the boundary of VP and the companion cell-sieve tube complex and subsequently uploading into the phloem of small and intermediate veins within source leaves.

The sucrose-export-defective maize plant was previously investigated by Russin et al. (1996). This *SXD-1* mutant was shown to develop abnormal accumulations of starch in BS cells, and anthocyanin pigments in the upper third of their leaves when compared

with *non-SXD-I-expressing* plants. These authors also clearly demonstrated that the upper portions of mutant source leaves contained abnormally high levels of starch in BS cells, which seem to distort the vascular bundles. These distorted veins were apparently not able to export sucrose and instead, the leaves accumulated an uncharacteristically high proportion of starch in BS chloroplasts. The basal portions of these leaves contrast sharply, they resemble the normal control leaves and were demonstrated to have near-normal export capacity.

Apparently, plasmodesmata at the BS-VP interface appeared to be structurally altered in the mutant leaves and occluded. Anthocyanin expression spread basipetally from the upper third of the leaves, and the leaves ultimately died within a week or two of visible anthocyanin expression. Russin et al. (1996) suggested that the structural alteration of the plasmodesmata was severe enough to potentially preclude symplasmic transport through these affected areas, and this could therefore account for the abnormal accumulation of starch and anthocyanin.

However, several issues remained unclear from this work. First, was there a possibility of plasmodesmally mediated transport across the BS-VP interface? Secondly, were there any normal but nonfunctional plasmodesmata at the BS-VP interface? Thirdly, was the lack of transport capacity indeed due to malformed plasmodesmata or perhaps due to a sucrose transport enzyme system malfunction at the companion cell-sieve element interface in the mutant?

The principal questions for us focussed upon the need to examine the ultrastructure related to transport capacity of plasmodesmata at the BS-VP interface. To this end, we utilized dye coupling experiments to explore intercellular movement of the symplasmically transported fluorescent dye Lucifer yellow (LYCH), after injection into the KMS-BS and BS-VP cell interfaces, using reverse current iontophoretic injection techniques. Specifically, we injected bundle sheath cells in loading veins from normal, nonexpressing as well as expressing leaf material. The hypothesis was that LYCH would be taken up and transferred from BS cells to the underlying phloem parenchyma cells, provided a symplasmic route existed.

We demonstrate that the transport bottleneck appears not to be due to malformed plasmodesmata as was suggested by Russin et al. (1996), but rather due to the deposition of callose at the BS-VP interface in the anthocyanin-rich (*SXD-I* mutant) leaf blade tissue and concomitantly, that the presence of callose coincided with a drop in symplasmic cell-to-cell transport across the BS-VP interface of maize mutant *SXD-I* leaf blades.

Materials and methods

Plant material

Zea mays L. seed of plants known to express the *SXD-I* mutation was kindly supplied by Pioneer Hi-Bred International, Johnston, Iowa, U.S.A. Control maize seed (*Z. mays* L. vat. 'early pearl') was obtained from Agricolor, Paarl Road Brackenfell, South Africa. Plants were grown in a mixture of potting soil and river sand, watered every second day and fertilized twice per week with Chemicult hydroponic nutrient powder (Starke-Ayres Pty Ltd, Eppindust, South Africa), which contained the following nutrients: 6.5% N, 2.7% R 13.0% K, 7% Ca, 2.2% Mg, and 7.5% S, and the following micronutrients: 0.15% Fe, 0.024% Mn, 0.005% Zn, 0.002% Cu, and 0.001% Mo. Plants were grown in a greenhouse under natural lighting conditions.

Since our primary interest was in comparison of control with mutant plants, several plantings using approximately 500 seeds in total were undertaken over several growing seasons, from which we were able to harvest a total of six plants that showed the *SXD-I* mutant syndrome.

Plants in which the *SXD-1* gene was not expressed are referred to as nonexpressing (they show no visible anthocyanin pigmentation). Plants that express the *SXD-1* gene (extensive anthocyanin-rich zones in leaf and sheath tissues) are referred to as expressing. See Russin et al. (1996) for a full explanation of the expression characteristics.

Electron microscopy

Small segments (each ca. 2 by 2 mm) were excised from leaf strips cut from the tip and basal regions of leaves (usually the fourth to sixth visible leaf, counting from the top) of control (nonmutant) and both expressing and *non-SXD-1-expressing* mutant tissues. In an effort to minimize callose formation in excised leaf segments, all tissue manipulation and fixation was undertaken at 4 °C in 6% glutaraldehyde in 0.05 M sodium cacodylate buffer (pH 7.2). The fixative was changed at least four times during a 5 h period, prior to dicing the leaf material into smaller (approximately 1 by 1 mm) pieces. After several cold-buffer rinses, the tissue pieces were postfixed overnight in 2% (w/v) osmium tetroxide in 0.05 M cacodylate buffer in a refrigerator. Following this, the tissue was dehydrated in a cold, graded ethanol series, followed by two 30 min changes of propylene oxide and finally infiltrated and embedded in an Araldite- Taab 812 resin mixture.

Thin (silver-gold) sections were cut with a diamond knife (Drukker International, Cuijk, the Netherlands) on an LKB (Bromma, Sweden) Ultratome III and collected on 300-mesh copper grids. These sections were stained with uranyl acetate (30 min) followed by lead citrate (5 min). Sections were viewed and photographed with a JEOL JEM-1210 transmission electron microscope (JEOL, Tokyo, Japan) at 80 kV or 100 kV. Approximately 80 nonserial sections each of nonexpressing and expressing leaf blade material was examined for plasmodesmal structure and possible malformation.

Electrophysiology and dye coupling studies

Microiontophoresis injections were conducted at specific points along the loading pathway in tip and basal segments of the leaf blade. As mentioned previously, we specifically focussed our injection studies on the KMS-BS and BS-VP interfaces.

Leaf tissue preparation

Long (ca. 5-7 cm) leaf strips were quickly but gently cut out from either the tip or basal regions of control or mutant plants and were immediately immersed in cold (ca. 6°C) MES buffer (10 mM NaOH-morpholinoethanesulfonic acid, pH 7.2), supplemented with KCl, MgCl₂, and CaCl₂ (all 0.5 mM) in 125 mM mannitol in petri dishes. Leaf strips were cut to include the midvein down one side of the section, in order to keep the leaf strip rigid while in MES buffer. After a period of not less than 30 min, the abaxial epidermis was gently scraped with a sharp single-edged razor blade to remove the cuticle and underlying epidermal tissue from the abaxial surface of the leaf strip in small areas (effectively opening "windows" into the mesophyll) in regions in which we intended to inject LYCH intercellularly. Once scraped, the leaf strips were allowed to acclimate in fresh MES buffer for at least 30 min before being used for injection experiments. The acclimated leaf strips were taped to glass microscope slides with a single-sided tape and submerged in Perspex slide wells, under MES buffer, and the slide well was transferred to the microscope.

Microscopic examination of LYCH iontophoretic experiments

An Olympus BHW1 (Olympus, Tokyo, Japan) upright-image fixed-stage UV microscope with a fixed stage and ultra-long working distance objectives (x10 and x25) was used to impale selected cells for the subsequent microinjection studies.

Electrophysiological measurements

Electrophysiological measurements were made with a WPI Duo 773 electrometer (World Precision Instruments Inc., Sarasota, Fla., U.S.A.) fitted with high-impedance, active probes. Essentially, the techniques described below are the same as developed by Kempers et al. (1997, 1999) and as described in Botha and Cross (1997).

Preparation of micropipettes

Inner-filamented glass micropipettes were made with 1 mm diameter pipettes (WPI K-series borosilicate capillaries, Kwik-Fil K100-F3), which were pulled with a Narishige PB-7 pipette puller (Narishige Co. Ltd, Tokyo, Japan). Pipettes generally had tips with diameters of approximately 0.5 μm or less. The micropipettes were back-filled with a LYCH (5%, w/v, in water) solution, and the shank was then back-filled with 3 M LiCl, taking care to avoid introducing air bubbles. The filled micropipettes were then carefully inserted into WPI LiCl half-cells which were filled with 3 M LiCl. The half-cells were attached to a WPI high-impedance probe, which was in turn attached to a WPI PM-10 Piezo controller unit fitted to a WPI DC-3 motorized micromanipulator.

Microinjections

The micropipette was manoeuvred into close proximity of the leaf surface with the tip immersed under the surface of the buffer, using the motorized micromanipulator described above. The measured current output of the WPI Duo 773 electrometer was set to zero at this stage, before the micropipette was advanced any closer to the immersed and exposed subepidermal tissues. Readings from -40 to -100 mV or lower indicated successful sealing of cells. After the cells had been impaled, the UV lamp shutter was inserted to minimize exposure and subsequent UV damage to the tissue. Once membrane potentials had stabilized, impaled cells were reverseiontophoresed, by application of current pulses (-2 to -30 nA) in 5-10 s pulses in order to inject the dye.

Image acquisition

Once the dye had been successfully iontophoresed and had been taken up, the micropipette was carefully withdrawn, and any LYCH-related transport was photographed on Fujichrome Provia 400 ASA slide film with an integral Olympus AD PM-10 camera system. Micrographs were taken immediately on successful injection and at various time intervals after the injections.

Fluorescence microscopy

Fresh tissue was prepared as for microiontophoresis and mounted in a 0.05% (w/v in water) aniline blue solution and viewed immediately with a Zeiss Standard Junior 18 microscope fitted with a Zeiss HBO 50 high-pressure mercury lamp (Carl Zeiss, Oberkochen, Federal Republic Germany). The microscope was fitted with a Zeiss MC63 photomicrography system. Specimens were viewed and photographed on Fujichrome Provia 400 ASA transparency film with either a Zeiss x25 (numerical aperture, 0.8), or x40 (numerical aperture, 0.9), oil-water-glycerine or a x63 (numerical aperture, 1.25) Plan Neofluar oil immersion objective.

Digital image preparation

Selected slides were scanned at 1200 pixels per inch resolution with a Nikon CoolScan II (Nikon Corporation, Tokyo, Japan) 35 mm slide scanner, and the images were saved as tagged information file format (TIFF) files. Adobe Photoshop 5.02 (Adobe Systems Incorporated, Mountain View, Calif., U.S.A.) was used to digitally enhance some of the images by Photoshop's edge enhancement filter, which effectively deconvolutes the fuzziness of fluorescence image edges.

Results

The principal results obtained in this study are illustrated in Figs. 1-7. In overview, only anthocyanin-expressing regions of the leaf blade (which occur in the assimilate-loading region) are incapable of LYCH transport between the BS and VP cells. Iontophoretic injection of BS cells in control (Fig. 1) and nonexpressing tissue (Fig. 2) clearly demonstrate that there is no impediment to symplasmic cell-to-cell transport, at

least between radial and longitudinal files of BS cells. Examination of the dye transport fronts to the right of the injection point in Fig. 1 shows that some transport was achieved to the tissues immediately endarch to the BS, and that VP cells appear to have taken up LYCH. Figures 1 and 2 clearly show lateral longitudinal and radial transfer into a cross vein in Fig. 1, and in Fig. 2 via the BS and VP cells, into an adjacent small vein. Note that the dye has moved into the underlying VP and has crossed over to an adjacent vein as well, but not out to the BS of the adjacent vein, and the dye front has been able to move some distance from the point of injection, and passed through a cross vein into an adjacent loading vein.

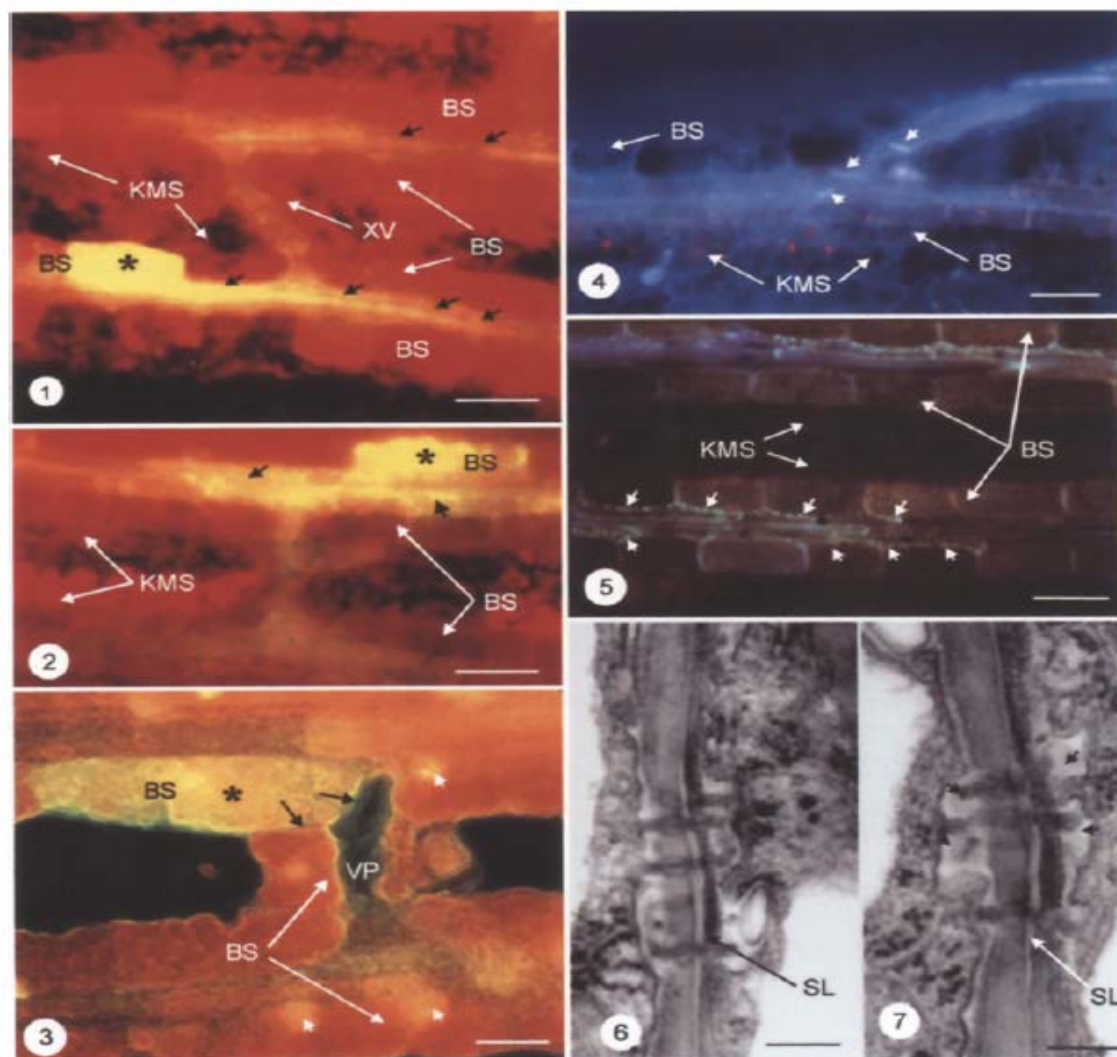
In contrast, expressing leaf tissues were not able to transport LYCH freely internal to the BS-VP interface. Our injection studies showed that transfer between BS cells was limited, and that transfer internally to VP was apparently not possible after injection in BS cells (Fig. 3). The faint green-yellow fluorescence in the VP of the cross vein may signify limited transfer of LYCH but contrasts sharply with the brightly fluorescing front at the injected BS cell, suggesting a major impediment to LYCH transport at this point. Areas of localized fluorescence occur in the BS cells.

Visualization of aniline blue-stained callose deposition

Figures 4 and 5 are fluorescence images taken of non-anthocyanin-expressing (Fig. 4) and anthocyanin-expressing (Fig. 5) leaf blade tissue, from which the abaxial leaf surface had been gently scraped (technique used was the same as that used for microinjection). These sections were examined immediately and again after 10-20 min under blue light with a fluorescence microscope (Fig. 4). Very little characteristic aniline blue-stained callose fluorescence was visible in non-anthocyanin-expressing tissue, other than that associated with the callose plugs (Fig. 4) characteristic of the sieve plates and pore-plasmodesmal areas in the phloem tissue. In sharp contrast to this, large numbers of fluorescing aggregates were seen at the BS-VP interface, immediately after bathing in aniline blue, in all anthocyanin-expressing leaf blade tissues. These fluorescence pinpoints (Fig. 5) correspond to the numerous plasmodesmal aggregates at this interface.

BS-VP plasmodesmal ultrastructure

Examination of the plasmodesmal fields at the BS-VP interfaces in nonmutant (Fig. 6) and anthocyanin-expressing (Fig. 7) leaf blade material shows that there is a more obvious and pronounced mix of electron-lucent and granular electron-dense deposit at the BS-VP interface of the anthocyanin-expressing material than of non-expressing leaf material. Plasmodesmata in Fig. 7 appear to be occluded. The areas of lucent and dense deposits correspond to the callose-rich areas seen under blue light in aniline blue-stained fresh material (Fig. 5).



Figs. 1–3. Leaf material after intercellular injection of LYCH. Asterisks mark the approximate points of injection in a BS cell. Images have been digitally enhanced with the edge filter in Adobe Photoshop, which has effectively sharpened the edges of otherwise slightly fuzzy fluorescence micrograph. Bars: Figs. 1 and 2, 200 μ m; Fig. 3, 50 μ m

Fig. 1. Two intermediate veins connected by a cross vein (*XV*) at center in a control leaf. Note extensive longitudinal transport from the injected BS cell into the underlying VP cells (short arrows) and evidence of transfer to the VP of the vein above, in a nonmutant leaf. *KMS* Kranz mesophyll

Fig. 2. Transport of LYCH longitudinally and internally to the underlying vascular parenchyma cells in a small vein (short arrows point to the longitudinal and radial transport to the VP underlying the injected BS cell) in a non-anthocyanin-expressing region of a mutant leaf. Evidence of some lateral transfer can be seen via the cross vein to the vein below

Fig. 3. Restricted transport in expressing mutant tissues. Note sharp discrimination of the fluorescent dye front in the injected BS cell (arrows). Whilst the VP of the cross vein appears slightly fluorescent, there is little evidence from this or other micrographs of transfer from the BS to VP cells in cross veins. Areas of localized fluorescence occur in some of the BS cells (arrowheads)

Figs. 4 and 5. Photomicrographs of control leaf tissue (Fig. 4) and expressing leaf tissue (Fig. 5), stained in aniline blue, showing distribution of callose deposition. In normal and also in non-anthocyanin-expressing control tissues (Fig. 4), callose was characteristically associated with the sieve plates as in this small vein. Note the absence of any callose deposits in the BS–VP interface in this micrograph. In contrast, Fig. 5 shows large aggregates of aniline blue-stained callose, seen here as pinpoints, and noticeably at the BS–VP interface. These fluorescence pinpoints correspond to the many plasmodesmal aggregates, which occur at high frequency at this interface. Arrowheads indicate callose-plugged sieve plate pores (Fig. 4) and plasmodesmal aggregates (Fig. 5). *BS* Bundle sheath; *KMS* Kranz mesophyll. Bars: 100 μ m

Figs. 6 and 7. Electron micrographs of plasmodesmata at the BS–VP interface in control (Fig. 6) and expressing leaf blade tissue. Note the compound suberin lamella (*SL*), which occurs between cells at this interface. Whilst the plasmodesmata in Fig. 6 appear normal, with characteristic neck constrictions, those in Fig. 7 appear malformed and occluded by amorphous electron-lucent and granular electron-dense material (arrowheads). These occlusions correspond to the fluorescent areas seen in Fig. 5. Bars: 300 nm

Discussion

Typical of all other grasses studied, the NADP-Me C⁴ *Z. mays* has high plasmodesmal frequencies at the KMS-BS and BS-VP interfaces (see Botha 1988; Botha and Cross 1997; Evert et al. 1977, 1996). The electron micrographs shown by Russin et al. (1996) present compelling evidence that there may be occlusions formed in, or blind plasmodesmata formed at, the BS-VP interface of *SXD-1* mutants. Our injection studies clearly demonstrate that there is rapid symplasmic transport and that connectivity exists between the KMS (not shown), and particularly between the BS and the VP in the minor veins of the leaf, in control and nonexpressing leaf tissue, but not in regions of the leaves that were positive anthocyanin-expressing *SXD-1* mutant material.

The low frequency with which the mutant syndrome appeared meant that relatively few (16 in all) leaves were available for this study. However, none of the sections examined showed evidence of malformed plasmodesmata at the BS-VP interface. Only one half plasmodesma was found during the course of our investigation, and this could possibly have been from an oblique section.

Anthocyanin accumulation has been suggested to be associated with excess carbohydrate accumulation in the BS cells of mutant leaves (Russin et al. 1996, Allison and Weinmann 1970). Soluble sugars are only converted into starch in the BS cells when the rate of sugar accumulation in the BS cells exceeds sugar export into the VP cells (Rhoades and Carvalho 1944). An accumulation of starch such as is expressed in the *SXD-1* maize mutant has also been observed in upper leaves of control maize plants where the ears, which are a major sink, have been removed (Allison and Weinmann 1970). When a major sink is removed, its demand for photosynthates is also removed, and so the photosynthates that would have supplied that sink are not exported from the leaf tissue, and similar to the *SXD-1* *Z. mays* mutant, it accumulates starch in the BS cells (see Russin et al. 1996). Such abnormal concentrations of nonstructural carbohydrates might well interfere with some of the functions of the leaf (Allison and Weinmann 1970). Clearly, plasmodesmal dysfunction or blockage would prevent transport and, hence, promote accumulation of starch for example.

Russin et al. (1996) suggested that the basipetal spread of anthocyanin accumulation in the *SXD-1* mutant leaf tissue is only a visible manifestation of the mutation. In other words, it was possible that green tissues near the *SXD-1* anthocyanin-expressing tissues could also express the mutation, albeit at states or levels of expression different from the anthocyanin-containing parts of the leaf blade. This idea is borne out in differences in the transport ability in *SXD-1*-expressing leaves, between the upper regions of the lamina, which contained anthocyanin, and the basal region, which was anthocyanin free. In these leaves, the tip did not export ¹⁴C-labelled photosynthates, whilst the basal leaf tissue retained variable transport capacity. The use of ¹⁴C label to localize sugar movement in control, nonexpressing (green), and the anthocyanin-expressing *SXD-1* mutant clearly demonstrated that ¹⁴C-labelled carbon transport was drastically reduced and long-distance transport out of the upper portion of the mutant leaves containing anthocyanin was severely impaired. Clearly, these experiments showed that after incorporation of carbon into sucrose in the BS, its loading through the VP to the companion cellsieve tube complex was adversely affected in the anthocyanin-expressing mutant. Thus, the ¹⁴C labeling data of Russin et al. (1996) together with our evidence for very limited LYCH transport from the BS to the VP (Fig. 3) suggest that the export capacity in the green

tissue within the mutant leaf seems to be variably affected, whilst in the anthocyanin-producing regions within the same leaf blade transport across the BS-VP interface is severely curtailed or prevented.

The very high plasmodesmal frequencies reported at the KMS-BS and BS-VP interfaces in control *Z. mays* (Evert et al. 1977) like other NADP-Me species (see Botha 1988 and references therein) suggests a symplasmic loading pathway. The ease of passage of LYCH across the KMS-BS-VP interface in control and green mutant leaf tissues supports our model of symplasmic transport of LYCH across the BS-VP interface, through open, symplasmically functional plasmodesmal channels.

Whilst not a major thrust of the research reported here, we assume that the interface between green, nonexpressing, and anthocyanin-expressing leaf tissues will have variable BS-VP transport capacity, as the LYCH injections attempted at the transition zone yielded varied limitation to transport across the BS-VP interface. Russin et al. (1996) suggested that a specific gene was implicated in the lack of transport and that it was in some way associated with, or regulated, plasmodesmal development (see also Ding et al. 1993 and references therein). However tempting, it is unlikely that a plasmodesmal wall occlusion mechanism is involved here. We saw no evidence for increased wall material deposition at or near plasmodesmal aggregates in nonexpressing or *SXD-1*-expressing mutant leaf blade material.

Nelson and Dengler (1997) stated that there is a clear need for a synchronized spatial and functional organization of cell types around the vascular system in leaves. The means by which this is achieved is, however, not well understood. A fundamental functional distinction has been suggested between the plasmodesmata in the mesophyll and vascular tissue. These plasmodesmata exist in two domains which are of different meristematic origin (Nelson and Dengler 1997, Ding 1998, Kollmann and Glockmann 1999). Plasmodesmata at the BS-VP interface thus traverse and interconnect these two domains. Interestingly, it is the BS-VP interface in soybean that presents a barrier to entry of cowpea chlorotic mottle virus (Goodrick et al. 1991) and also of tomato aspermy virus in *Cucumis sativus* (Thompson and Garcia-Arenal 1998); in both instances preventing access to the phloem. It is also of interest to note that transgenic tobacco plants that express the 30kDa movement protein of tobacco mosaic virus (essential for the distribution of tobacco mosaic virus) localize the movement protein only in the plasmodesmata of the nonvascular cells (Ding et al. 1992). The tobacco mosaic virus movement protein transgenic plants were found to contain sucrose, fructose, glucose, and starch at levels considerably higher than those in control plants (Lucas et al. 1993), suggesting some form of plasmodesmal gating.

When freshly prepared mutant leaf blade material treated with aniline blue was examined under blue light, callose was observed in association with the plasmodesmal fields at the BS-VP interface in anthocyanin-expressing leaf blade tissue. The large array of callose deposits at the BS-VP interface in Fig. 5 is overwhelming evidence for callose localization at or near plasmodesmata (see Figs. 6 and 7). These deposits were absent in control and non-anthocyanin-expressing *SXD-1* mutant leaf tissue. Lack of, or highly reduced, LYCH transport in anthocyanin-expressing *SXD-1* leaf blade material is supported by iontophoretic injections such as that shown in Fig. 3, where a sharp contrast exists between the LYCH-containing BS cell and the VP cell associated with the cross vein, suggesting that the plasmodesmata at the BS-VP interface were occluded. It is this interface that is involved in plasmodesmal blockage in the *SXD-1* maize mutant and which causes a decreased phloem loading capacity.

Transport of ions and metabolites through plasmodesmata is thought to be controlled at the neck region, due to the constriction of the cytoplasmic annulus and the deposition of callose (Radford et al. 1998). Radford et al. (1998) demonstrated the inhibition of callose formation in *Allium cepa* roots through incubation of the plant tissue with 2-deoxy-D-glucose for 1 h prior to fixation in 2.5% glutaraldehyde. Radford et al. (1998) suggested that the neck constrictions and raised collars seen in conventional electron micrographs are artefacts due to physical wounding and glutaraldehyde fixation. However, we find no evidence for wounding effects in *Z. mays* leaf blade tissue under the experimental conditions reported here. Clearly, the disparity between the positive transport capacity in nonexpressing and the nonexistent transport capacity in expressing *Z. mays* leaf material cannot be accounted for simply as a wounding effect, which would logically have affected all tissues, and not just the *SXD-1* anthocyanin-expressing mutant exclusively. That callose was visible immediately after addition of aniline blue in the anthocyanin-rich *SXD-1* *Z. mays* leaf tissue (see Fig. 5) advocates prior presence, and not formation due to wounding as postulated for other tissues (Blackman et al. 1998, Radford et al. 1998). In all sections of nonexpressing leaf tissue examined for callose, little if any callose deposition was visualized at the BS-VP interface even 20 min after wounding through scraping (Fig. 4). The lack of callose formation at the BS-VP interface in nonanthocyanin-expressing tissues negates argument for a wound response. Calcium has been implicated and identified as a major factor in the regulation of intercellular communication via plasmodesmata (Beebe and Turgeon 1991 and references therein; Schulz 1999; Tucker and Boss 1996). Calcium has been reported elsewhere to influence callose synthesis (Robards and Lucas 1990 and references therein). Dye coupling experiments carried out with increased cytosolic Ca^{++} levels have shown that there is a significant decrease in movement of dye molecules when Ca^{++} levels are elevated (see Erwee and Goodwin 1983, Robards and Lucas 1990). Apitius and Lehmann (1995) suggested that cells of the liverwort *Riella heliophylla* could be physiologically wounded and that this wound stimulation induced calcium-mediated callose deposition on the cell walls within 10 min after wounding. Schulz (1999) suggests that increasing calcium ion concentration induces closure of the cytoplasmic gateway by plasmodesmatal proteins. Schulz (1999) further suggests that if Ca^{++} remains at a high level, callose synthesis becomes activated, and the result is permanent closure of the plasmodesmal canals, supporting the earlier finding by Tucker (1990) where lasting high levels of Ca^{++} apparently induced long-term functional closure of plasmodesmata. We show clear evidence for the presence of callose at the BS-VP interface but only in anthocyanin-expressing portions of mutant leaf tissue. Blockage or gating of the plasmodesmata at the BS-VP interface must adversely affect symplasmic transport across this important interface resulting in a major decline in symplasmic transport. Clearly, callose deposition is linked in some way to the expression of the *SXD-1* mutation in *Z. mays*. Perhaps expression of the *SXD-1* mutation is, in some way, linked to changes in Ca^{++} levels in the cytosol.

Acknowledgments

C.E.J.B. acknowledges the financial support of the National Research Foundation (formally the Foundation for Research Development), Pretoria, South Africa, as well as the Joint Research Committee, Rhodes University, for their continued financial support and equipment grants, which made this work possible. We express our sincere thanks to Dr. Ronald Kempers (previously in A.J.E.v.B.'s laboratory, now at Molecular Probes, Leiden, the Netherlands), who gave so freely of his time and expertise during the early stages of

our microinjection efforts. We acknowledge the excellent technical assistance with some of the microinjection experiments provided by Miss Inge von Senger. We gratefully acknowledge the Management of Pioneer Hi Bred in the United States for kindly making SXD-1 seed available to us.

References

- Allison JCS, Weinmanu H (1970) Effect of absence of developing grain on carbohydrate content and senescence of maize leaves. *Plant Physiol* 46:435-436
- Apitius A, Lehmann H (1995) The deposition of different wall materials as a wound reaction in the liverwort *Riella helicophylla*. *Cryptogam Bot* 5:351-359
- Beebe DU, Turgeon R (1991) Current perspectives on plasmodesmata structure and function. *Physiol Plant* 83:194-199
- Blackman LM, Gunning BES, Overall RL (1998) A 45 kDa protein isolated from the nodal walls of *Chara corallina* is localised to plasmodesmata. *Plant J* 15:401-411
- Botha CEJ (1988) Plasmodesmatal distribution and frequency in vascular bundles and contiguous tissue of the leaf of *Themeda triandra*. *Planta* 173:433-441
- Cross RHM (1997) Plasmodesmatal frequency in relation to short-distance transport and phloem loading in the leaves of barley (*Hordeum vulgare*): phloem is not loaded directly from the symplast. *Physiol Plant* 99:355-362
- Ding B (1998) Intercellular protein trafficking through plasmodesmata. *Plant Mol Biol* 38:279-310
- Haudenschild JS, Hull RJ, Wolf S, Beachy RN, Lucas WJ (1992) Secondary plasmodesmata are specific sites of localization of the tobacco mosaic movement protein in transgenic tobacco plants. *Plant Cell* 4:915-928
- - Willmitzer L, Lucas WJ (1993) Correlation between arrested secondary plasmodesmal development and the onset of accelerated leaf senescence in yeast acid invertase transgenic plants. *Plant J* 4: 179-189.
- Erwee MG, Goodwin PB (1983) Characterisation of the *Egeria densa* Planch. leaf symplast: inhibition of the intercellular movement of fluorescent probes by group II ions. *Planta* 158:320-328
- Evert RF, Eschrich W, Heyser W (1977) Distribution and structure of plasmodesmata in mesophyll and bundle-sheath cells of *Zea mays*. *Planta* 136:77-89
- - - (1978) Leaf structure in relation to solute transport and phloem loading in *Zea mays* L. *Planta* 138:279-294
- Russin WA, Botha CEJ (1996) Distribution and frequency of plasmodesmata in relation to photoassimilate pathways and phloem loading in the barley leaf. *Planta* 198:572-579
- Gamalei YV (1989) Structure and function of leaf minor veins in trees and herbs: a taxonomic review. *Trees* 3:96-110
- (1991) Phloem loading and its development related to plant evolution from trees to herbs. *Trees* 5:50-64
- Goodrick B J, Kuhn CW, Hussey RS (1991) Restricted systemic movement of cowpea chlorotic mottle virus in soybean with non-necrotic resistance. *Phytopathology* 81:1426-1431
- Hughes JE, Gunning BES (1980) Glutaraldehyde-induced deposition of callose. *Can J Bot* 58:250-258
- Kalt-Torres W, Kerr PS, Usuda H, Huber SC (1987) Diurnal changes in maize leaf photosynthesis. *Plant Physiol* 83:283-288
- Kempers R, van Bel AJE (1997) Symplasmic connections between sieve element and companion cell in the stem phloem of *Vicia faba* L have a molecular exclusion limit of at least 10 kDa. *Planta* 201:195-200
- Prior DAM, Oparka KJ, Knoblauch M, van Bel AJE (1999) Integration of controlled intercellular pressure injection, iontophoresis and membrane potential measurement. *Plant Biol* 1:61~67
- Kollmann R, Glockmann C (1999) Multimorphology and nomenclature of plasmodesmata in higher plants. In: van Bel AJE, van Kesteren WJP (eds) *Plasmodesmata: structure, function, role in cell communication*. Springer, Berlin Heidelberg New York Tokyo, pp 149-172
- Lucas WJ, Olesinski A, Hull RJ, Haudenschild JS, Deom CM, Wolf S, Beachy RN (1993) Influence of the tobacco mosaic virus 30-kDa movement protein on carbon metabolism and photosynthate partitioning in transgenic tobacco plants. *Planta* 190:88-96
- Nelson T, Dengler N (1997) Leaf vascular pattern formation. *Plant Cell* 9:1121-1135
- Radford JE, Vesk M, Overall RL (1998) Callose deposition at plasmodesmata. *Protoplasma* 201:30-37
- Rhoades MM, Carvalho A (1944) The function and structure of the parenchyma sheath plastids of the maize leaf. *Bull Torrey Bot Club* 71:335-346
- Robards AW, Lucas WJ (1990) Plasmodesmata. *Annu Rev Plant Physiol Plant Mol Biol* 41:369-419

- Russin WA, Evert RF, Vanderveer P J, Sharkey TD, Briggs SP (1996) Modification of a specific class of plasmodesmata and loss of sucrose export ability in the sucrose export defective1 maize mutant. *Plant Cell* 8:645-658
- Schulz A (1999) Physiological control of plasmodesmal gating. In: van Bel AJE, van Kesteren WJP (eds) *Plasmodesmata: structure, function, role in cell communication*. Springer, Berlin Heidelberg New York Tokyo, pp 173-204
- Thompson JR, Garcia-Arenal F (1998) The bundle-sheath phloem interface of *Cucumis sativus* is a boundary to systemic infection by tomato aspermy virus. *Mol Plant Microbe Interact* 11: 109-114
- Tucker EB (1990) Calcium-loaded 1,2-bis(2-aminophenoxy)ethane- N,N,N',N'-tetra acetic acid blocks cell-to-cell diffusion of carboxyfluorescein in staminal hairs of *Setcreasea purpurea*. *Protoplasma* 174:45-49
- Boss WF (1996) Mastoparan-induced intracellular Ca²⁺ fluxes may regulate cell-to-cell communication in plants. *Plant Physiol* 111:459-467
- Turgeon R, Beebe DU (1991) The evidence for symplasmic phloem loading. *Plant Physiol* 96:349-354
- van Bel AJE (1992) Different phloem-loading machineries correlated with the climate. *Acta Bot Neerl* 41:121-141
- (1993) Strategies of phloem loading. *Annu Rev Plant Physiol Plant Mol Biol* 44:253-281